

Confinement-induced enhancement of superconductivity in a spin- $\frac{1}{2}$ fermion chain coupled to a \mathbb{Z}_2 lattice gauge field

Zi-Yong Ge¹ and Franco Nori^{1,2,3}

¹*Theoretical Quantum Physics Laboratory, Cluster for Pioneering Research, RIKEN, Wako-shi, Saitama 351-0198, Japan*

²*Center for Quantum Computing, RIKEN, Wako-shi, Saitama 351-0198, Japan*

³*Department of Physics, University of Michigan, Ann Arbor, Michigan 48109, USA*

 (Received 17 August 2022; revised 15 February 2023; accepted 7 March 2023; published 21 March 2023)

We investigate a spin- $\frac{1}{2}$ fermion chain minimally coupled to a \mathbb{Z}_2 gauge field. In the sector of the gauge generator $\hat{G}_j = -1$, the model reduces to the Hubbard model with repulsive on-site interaction coupled to a \mathbb{Z}_2 gauge field. We uncover how electric fields affect low-energy excitations by both analytical and numerical methods. In the half-filling case, despite electric fields, the system is still a Mott insulator, just like the Hubbard model. For hole-doped systems, holes are confined under nonzero electric fields, resulting in a hole-pair bound state. Furthermore, this bound state also significantly affects the superconductivity, which manifests itself in the emergence of attractive interactions between bond-singlet Cooper pairs. Specifically, numerical results reveal that the dimension of the dominant superconducting order parameter becomes smaller when increasing the electric field, signaling an enhancement of the superconducting instability induced by lattice fermion confinement. The superconducting order can even be the dominant order of the system for suitable doping and large applied electric field. The confinement also induces a π momentum for the dominant superconducting order parameter leading to a quasi-long-range pair density wave order. Our results provide insights for understanding unconventional superconductivity in \mathbb{Z}_2 lattice gauge theories and might be experimentally addressed in quantum simulators.

DOI: [10.1103/PhysRevB.107.125141](https://doi.org/10.1103/PhysRevB.107.125141)

I. INTRODUCTION

Lattice gauge theories (LGTs) were originally proposed to understand the confinement of quarks and became a fundamental concept in high-energy physics [1]. In correlated electronic systems, due to strong quantum fluctuations, LGTs can also emerge leading to many exotic quantum phases [2–7]. Moreover, LGTs have also been applied to understand high- T_c superconductors, where $U(1)$ [8], $SU(2)$ [9,10], and \mathbb{Z}_2 [11] gauge theories have been introduced in doped Mott insulators [12–14]. However, studying LGTs coupled to dynamical matter fields, especially in the two-dimensional (2D) case, is a quite challenging task for conventional methods. Explicitly, there is a sign problem for quantum Monte Carlo methods [15–17], and the density matrix renormalization group (DMRG) [18–20] method is difficult to extend to high-dimensional systems due to large entanglement entropies. Recently, with the rapid development of quantum simulations [21–27], studying LGTs in synthetic quantum many-body systems has become possible [28–47]. Quantum simulations provide an alternative for understanding or solving hard problems in LGTs. Meanwhile, quantum simulators are also an outstanding platform to study nonequilibrium dynamics of LGTs [48–50].

The simplest example of LGTs is \mathbb{Z}_2 gauge theories [2,5,51,52]. Motivated by recent quantum simulation experiments, studying \mathbb{Z}_2 LGTs coupled to dynamical matter fields has attracted considerable interests [53–68]. These works mainly focus on single-component matter fields. However, to relate to unconventional superconductors, spin- $\frac{1}{2}$ (two-component) fermions should be considered as the matter

field. Generally, there exists different low-energy physics between single- and multicomponent fermions coupled to gauge fields. For instance, deconfined phases are absent in 2D single-component fermions coupled to \mathbb{Z}_2 LGTs, while they can emerge in two- or multicomponent cases [69,70]. However, \mathbb{Z}_2 LGTs coupled to spin- $\frac{1}{2}$ fermions are not yet fully understood even in one dimension, especially the superconducting order in the sector of the gauge generator $\hat{G}_j = -1$ with doped holes [11,70,71]. Moreover, it is still an open question how to realize this system in quantum simulators.

In this paper, we present systematic investigations of a spin- $\frac{1}{2}$ fermion chain coupled minimally to a \mathbb{Z}_2 LGT. To relate to the physics of Mott insulators and unconventional superconductors, we mainly consider low-energy excitations in the $\hat{G}_j = -1$ sector. Thus, the system is equivalent to the Hubbard model coupled to a \mathbb{Z}_2 gauge field. The presence of an electric field term induces a nonvanishing expectation value of electric field and a large fluctuation of gauge field. Therefore, strings formed between charges are made of stable electric fields leading to the confinement of lattice fermions. We first present a phenomenological analysis of the ground state and derive the effective Hamiltonian in the large electric field limit. The half-filling system is still a Mott insulator with the spin sector being an antiferromagnetic Heisenberg model. Hence, similar to the Hubbard model, there is a deconfined spinon excitation, although lattice fermions are confined. However, in hole-doped systems, the electric field can induce confinement of holes resulting in the emergence of hole-pair bound states. Moreover, the kinetic term of the hole pair can contribute to an attractive interaction between

bond-singlet Cooper pairs, which is expected to enhance the superconductivity.

We also implement DMRG [18–20] methods to support the above analytical discussion. Numerical results demonstrate that lattice fermions are indeed always confined in half-filling systems, whereas they become deconfined in hole-doped systems when electric fields are absent. In addition, there exists a deconfined spinon excitation in both half-filling and hole-doped cases, just like the Hubbard model. Regarding superconductivity, we find that bond-singlet pairs are the dominant superconducting order parameter in hole-doped systems. Remarkably, the dimension of this order parameter becomes smaller when increasing an applied electric field, revealing that the confinement of holes can enhance superconductivity. Meanwhile, the superconducting order can be the dominant order of the system for large applied electric field and suitable doping. Numerical results also show that the confinement can result in a π momentum for the dominant superconducting order. Thus, there exists a quasi-long-range pair density wave (PDW) correlation [72–77]. Finally, we also propose an approach to implement our model in experimental quantum simulators.

The rest of this paper is organized as follows. In Sec. II, we introduce the model of a one-dimensional (1D) spin- $\frac{1}{2}$ fermion chain coupled to a \mathbb{Z}_2 gauge field. In Sec. III, we present a phenomenological discussion about the confinement of lattice fermions and the existence of hole-pair bound states. In Sec. IV, we derive the effective Hamiltonian of the system with large electric fields, and analyze how hole-pair bound states enhance the superconducting order. In Sec. V, we present numerical results calculated by DMRG methods to support the above discussion. A possible experimental implementation of this system is proposed in Sec. VI. Finally, in Sec. VII, we summarize the results and give an outlook of our paper.

II. MODEL

Here we consider a spin- $\frac{1}{2}$ fermion chain coupled to a dynamical \mathbb{Z}_2 gauge field. The Hamiltonian reads

$$\begin{aligned} \hat{H} = & -t \sum_{j=1}^{L-1} \sum_{\sigma=\uparrow,\downarrow} (\hat{f}_{j,\sigma}^\dagger \hat{\tau}_{j+\frac{1}{2}}^z \hat{f}_{j+1,\sigma} + \text{H.c.}) \\ & - h \sum_{j=1}^L \hat{\tau}_{j+\frac{1}{2}}^x - \frac{U}{4} \sum_{j=1}^{L-1} \hat{\tau}_{j-\frac{1}{2}}^x \hat{\tau}_{j+\frac{1}{2}}^x, \end{aligned} \quad (1)$$

where $\hat{f}_{i,\sigma}^\dagger$ ($\hat{f}_{j,\sigma}$) is the creation (annihilation) operator of the fermion living on site j , $\hat{\tau}_{j+\frac{1}{2}}^\alpha$ is the Pauli matrix acting on the link between sites j and $(j+1)$ [labeled by $(j+\frac{1}{2})$], and L is the system size. The first term describes fermions coupled minimally to gauge fields via the Ising version of the Peierls substitution with amplitude $t > 0$. The second term is an electric field with strength $h > 0$. The third term is a ferromagnetic Ising interaction of electric fields with strength $U > 0$.

The Hamiltonian \hat{H} is \mathbb{Z}_2 gauge invariant with a generator defined as

$$\hat{G}_j = \hat{\tau}_{j-\frac{1}{2}}^x (-1)^{\hat{N}_j} \hat{\tau}_{j+\frac{1}{2}}^x, \quad (2)$$

where $\hat{N}_j = \hat{n}_{j,\uparrow} + \hat{n}_{j,\downarrow}$ ($\hat{n}_{j,\sigma} = \hat{f}_{j,\sigma}^\dagger \hat{f}_{j,\sigma}$) is the fermion number on site j . In addition to gauge invariance, \hat{H} also possesses a global $SU_s(2) \times U(1)$ symmetry for the arbitrary filling factor. Here $U(1)$ represents the conservation of total fermion number, i.e., $[\sum_j \hat{N}_j, \hat{H}] = 0$, and $SU_s(2)$ corresponds to the spin rotation. Specifically, for the half filling, due to the particle-hole symmetry, this continuous symmetry is enlarged to $SU_s(2) \times SU_\eta(2) \times U(1)$, where $SU_\eta(2)$ is the pseudospin rotation symmetry [78,79].

The 2D version of Eq. (1) in the $\hat{G}_j = -1$ sector is potentially relevant for understanding superconductivity in doped Mott insulators [11]. However, this is challenging for conventional numerical and analytic methods [69,70]. In the following, we will demonstrate that the 1D case can be addressed analytically by perturbation theory in the strong electric field limit. To relate to the physics of Mott insulators and superconductivity, we focus on the $\hat{G}_j = -1$ gauge sector. Thus, the Ising interaction of gauge fields under this gauge constraint is equivalent to an on-site repulsive interaction of fermions:

$$-\hat{\tau}_{j-\frac{1}{2}}^x \hat{\tau}_{j+\frac{1}{2}}^x = (1 - 2\hat{n}_{j,\uparrow})(1 - 2\hat{n}_{j,\downarrow}). \quad (3)$$

Therefore, the Hamiltonian (1) reduces to a Hubbard model when $h = 0$. Hereafter, we mainly study how electric fields affect the low-energy physics of the Hubbard model.

III. CHARGE CONFIGURATIONS OF GROUND STATES

To shed light on how the confinement of lattice fermions occurs, we first analyze phenomenologically the configuration of the charge sector in ground states. For simplicity, we can consider the limit $h, U \gg t$, where the terms

$$\hat{H}_h := -h \sum_{j=1}^L \hat{\tau}_{j+\frac{1}{2}}^x \quad (4)$$

and

$$\hat{H}_U := -\frac{U}{4} \sum_{j=1}^{L-1} \hat{\tau}_{j-\frac{1}{2}}^x \hat{\tau}_{j+\frac{1}{2}}^x \quad (5)$$

dominate the energy.

In the half-filling case, if each site occupies one fermion, then under the gauge constraint $\hat{G}_j = -1$, all τ spins can be polarized at $\langle \hat{\tau}_{j+\frac{1}{2}}^x \rangle = 1$, simultaneously. This configuration can indeed minimize the energy of both \hat{H}_h and \hat{H}_U . In addition, exciting a double occupation and a hole, which can be considered as a meson, at least costs energy $\sim(h+U)$, i.e., there is a charge gap. Thus, the system is still a Mott insulator identical to the Hubbard model, and lattice fermions $\hat{f}_{j,\sigma}$ should be confined. Here, the existence of electric fields can only enlarge the charge gap, but cannot change the Mott insulator phase in this case. We note that the situation becomes different when $U < 0$, describing antiferromagnetic

interactions of electric fields (or attractive on-site interactions of fermions) in the gauge sector $\hat{G}_j = -1$.

In Appendix C, we present a detailed discussion for $U < 0$. We find that there exists a quantum phase transition from the Mott insulator (gapless) to a meson condensed phase (gapped) when increasing $-U$. Here, the meson condensed phase spontaneously breaks the translational symmetry, and the corresponding matter field is a pseudospin valence-bond solid.

In hole-doped systems, it is not possible for each site to be occupied by a fermion, so not all τ spins can be polarized at $\langle \hat{\tau}_{j+\frac{1}{2}}^x \rangle = 1$ in the $\hat{G}_j = -1$ sector. In addition, double occupation should also be suppressed due to its energy cost $\sim (h + U)$. Thus, only holes and single-occupation states are allowed in the ground state. To reveal the configuration of the charge sector, we take the case of two holes as an example (to fix the even fermion parity subspace, we only consider an even number of holes). The corresponding gauge-invariant configuration has the form

$$|\dots + 1 + 0 - 1 - 1 - \dots - 1 - 1 - 0 + 1 + 1 + \dots\rangle, \quad (6)$$

where $|\pm\rangle$ labels the eigenstate of $\hat{\tau}^x$ with eigenvalue ± 1 , and $|0\rangle$ ($|1\rangle$) labels a hole (single occupation). In Eq. (6), there are r links polarized at the state $|-\rangle$, where r is the distance between two holes. Thus, there is a string tension between two holes with energy hr , so the hole becomes confined when $h \neq 0$. For large h , to minimize the energy, these two holes should be bonded on two nearest-neighbor (NN) sites. Generalizing to the multihole systems, we can find that holes must exist in pairs, i.e., form hole-pair bound states $|0-0\rangle$, which are absent in the Hubbard model. Therefore, in the presence of doped holes, the existence of \hat{H}_h can significantly affect the charge degrees of freedom, resulting in a distinct low-energy physics from the Hubbard model.

IV. EFFECTIVE HAMILTONIAN IN THE STRONG ELECTRIC FIELD LIMIT

To further uncover the effect of electric fields, we can consider the effective Hamiltonian in the limit of strong electric field $h \gg t$ and $U \rightarrow 0$. Using the Schrieffer-Wolf transformation [80,81], we can obtain

$$\hat{H}_{\text{eff}} = \hat{H}_h + \hat{H}_S + \hat{H}_K,$$

$$\begin{aligned} \hat{H}_S &= J \sum_j \hat{\tau}_{j+\frac{1}{2}}^x \cdot (\hat{s}_j \cdot \hat{s}_{j+1} + \hat{\eta}_j \cdot \hat{\eta}_{j+1}), \\ \hat{H}_K &= \frac{J}{2} \sum_{j,\sigma} \hat{\tau}_{j+\frac{1}{2}}^x \cdot (\hat{\tau}_{j-\frac{1}{2}}^z \hat{\tau}_{j+\frac{1}{2}}^z + \hat{\tau}_{j-\frac{1}{2}}^y \hat{\tau}_{j+\frac{1}{2}}^y) (\hat{f}_{j-1,\sigma}^\dagger \hat{f}_{j+1,\sigma} - \text{H.c.}), \end{aligned} \quad (7)$$

where the effective coupling $J = t^2/h$. In addition, $\hat{s}_j = (\hat{s}_j^x, \hat{s}_j^y, \hat{s}_j^z)$ is the spin operator defined as

$$\hat{s}_j := \sum_{\alpha,\beta} \hat{f}_{j,\alpha}^\dagger \boldsymbol{\sigma}_{\alpha\beta} \hat{f}_{j,\beta}, \quad (8)$$

where $\boldsymbol{\sigma}$ are Pauli matrices, and $\hat{\eta}_j = (\hat{\eta}_j^x, \hat{\eta}_j^y, \hat{\eta}_j^z)$ is the pseudospin operator generated by [78,79]

$$\hat{\eta}_j^\dagger = \hat{\eta}_j^x + i\hat{\eta}_j^y = (-1)^j \hat{f}_{j,\uparrow}^\dagger \hat{f}_{j,\downarrow}^\dagger, \quad (9)$$

Detailed derivations of Hamiltonian (7) are presented in Appendix A.

In the case of half filling, as discussed in Sec. III, all links are nearly polarized at $\langle \hat{\tau}_{j+\frac{1}{2}}^x \rangle = 1$, and each site occupies one fermion. Thus we have

$$\hat{\eta}_j \cdot \hat{\eta}_{j+1} = \hat{\tau}_{j-\frac{1}{2}}^z \hat{\tau}_{j+\frac{1}{2}}^z + \hat{\tau}_{j-\frac{1}{2}}^y \hat{\tau}_{j+\frac{1}{2}}^y = 0. \quad (10)$$

The effective Hamiltonian in this case is reduced to a 1D antiferromagnetic Heisenberg model (the constant is neglected):

$$\hat{H}_{\text{eff}}^{\text{HF}} = J \sum_j \hat{s}_j \cdot \hat{s}_{j+1}. \quad (11)$$

This is identical to the Hubbard model with large repulsive on-site interactions. Therefore, in addition to the charge sector, the electric field cannot affect the physics of the spin sector for the half filling. According to properties of the 1D Heisenberg model [4,12,82], there will be a deconfined spinon excitation. The spin operator \hat{s}_j is indeed gauge invariant, so this spinon excitation is physically allowed.

For hole-doped systems, since double occupations are still forbidden, according to Eq. (9), the term $\hat{\eta}_j \cdot \hat{\eta}_{j+1}$ only contributes a density-density interaction. The Heisenberg term $\hat{s}_j \cdot \hat{s}_{j+1}$ cannot vanish, if and only if the NN sites j and $(j+1)$ are both occupied by a single fermion, which corresponds to the link $(j+\frac{1}{2})$ for the state $|+\rangle$. Thus, $\hat{\tau}_{j+\frac{1}{2}}^x \cdot (\hat{s}_j \cdot \hat{s}_{j+1})$ is equivalent to $\hat{s}_j \cdot \hat{s}_{j+1}$, which is also gauge invariant. Thus, the effective Hamiltonian can be written as

$$\begin{aligned} \hat{H}_{\text{eff}}^{\text{HD}} &= J \sum_j (\hat{s}_j \cdot \hat{s}_{j+1} + \hat{N}_j \hat{N}_{j+1}) \\ &+ \frac{J}{2} \sum_{j,\sigma} \hat{\tau}_{j+\frac{1}{2}}^x \cdot (\hat{\tau}_{j-\frac{1}{2}}^z \hat{\tau}_{j+\frac{1}{2}}^z + \hat{\tau}_{j-\frac{1}{2}}^y \hat{\tau}_{j+\frac{1}{2}}^y) \\ &\times (\hat{f}_{j-1,\sigma}^\dagger \hat{f}_{j+1,\sigma} - \text{H.c.}). \end{aligned} \quad (12)$$

The second term in $\hat{H}_{\text{eff}}^{\text{HD}}$ is the next-nearest-neighbor (NNN) hopping term of holes. If the site j is a single-occupation state, then $\langle \hat{\tau}_{j-\frac{1}{2}}^x \rangle = \langle \hat{\tau}_{j+\frac{1}{2}}^x \rangle = 1$, leading to $\hat{\tau}_{j-\frac{1}{2}}^z \hat{\tau}_{j+\frac{1}{2}}^z + \hat{\tau}_{j-\frac{1}{2}}^y \hat{\tau}_{j+\frac{1}{2}}^y = 0$. If the site j is a hole, then $\langle \hat{\tau}_{j-\frac{1}{2}}^x \rangle = -\langle \hat{\tau}_{j+\frac{1}{2}}^x \rangle$ and $\hat{\tau}_{j-\frac{1}{2}}^z \hat{\tau}_{j+\frac{1}{2}}^z = \hat{\tau}_{j-\frac{1}{2}}^y \hat{\tau}_{j+\frac{1}{2}}^y \neq 0$. Thus, the NNN hopping of holes between $(j-1)$ and $(j+1)$ can contribute, if and only if the site in between is also a hole. That is, this term allows a hole-pair bound state $|0-0\rangle$ to hop to NN sites (see Fig. 1). Therefore, in the hole-doped system, the dynamics of the charge sector is contributed by hole pairs, while the spin sector is still an antiferromagnetic Heisenberg model. We further analyze the kinetic term \hat{H}_K to uncover how the hole-pair bound state affects the superconductivity. Here, $\langle \hat{\tau}_{j-\frac{1}{2}}^x \rangle = -\langle \hat{\tau}_{j+\frac{1}{2}}^x \rangle$, if site j is a hole, and $\langle \hat{\tau}_{j+\frac{1}{2}}^x \rangle = \pm 1$ with a hole pair at the link $(j \pm \frac{1}{2})$. Thus, H_K can be simplified as

$$\hat{H}_K = J \sum_{j,\sigma} \hat{f}_{j-1,\sigma}^\dagger \hat{\tau}_{j-\frac{1}{2}}^z \hat{\tau}_{j+\frac{1}{2}}^z \hat{f}_{j+1,\sigma} + \text{H.c.} \quad (13)$$

In addition, since the site j should be a hole, we can insert a term $\hat{f}_{j,\sigma} \hat{f}_{j,\sigma}^\dagger$ into Eq. (13). Therefore, this term can be

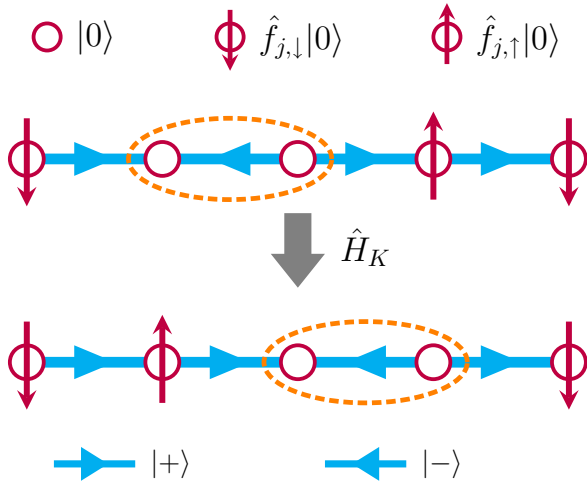


FIG. 1. Diagram of the hole-pair dynamics. The orange dashed ellipses represent a hole-pair bound state $|0-0\rangle$, which can hop to NN bonds under the action of \hat{H}_K .

rewritten as interactions of bond Cooper pairs:

$$\begin{aligned} \hat{H}_K &= J \sum_j \hat{\Phi}_{1,0}(j-1)\hat{\Phi}_{1,0}^{\dagger}(j) - \hat{\Phi}_{0,0}(j-1)\hat{\Phi}_{0,0}^{\dagger}(j) + \text{H.c.} \\ &= J \sum_j \hat{\Phi}_{1,\uparrow}(j-1)\hat{\Phi}_{1,\uparrow}^{\dagger}(j) + \hat{\Phi}_{1,\downarrow}(j-1)\hat{\Phi}_{1,\downarrow}^{\dagger}(j) + \text{H.c.}, \end{aligned} \quad (14)$$

where $\hat{\Phi}_{s,m}^{\dagger}$ ($s = 0, 1$ and $m = 0, \uparrow, \downarrow$) is the gauge-invariant order parameter of bond Cooper pairs with the form

$$\begin{aligned} \hat{\Phi}_{0,0}^{\dagger}(j) &:= \frac{1}{\sqrt{2}} \hat{\tau}_{j+\frac{1}{2}}^z (\hat{f}_{j,\uparrow}^{\dagger} \hat{f}_{j+1,\downarrow}^{\dagger} - \hat{f}_{j,\downarrow}^{\dagger} \hat{f}_{j+1,\uparrow}^{\dagger}), \\ \hat{\Phi}_{1,0}^{\dagger}(j) &:= \frac{1}{\sqrt{2}} \hat{\tau}_{j+\frac{1}{2}}^z (\hat{f}_{j,\uparrow}^{\dagger} \hat{f}_{j+1,\downarrow}^{\dagger} + \hat{f}_{j,\downarrow}^{\dagger} \hat{f}_{j+1,\uparrow}^{\dagger}), \\ \hat{\Phi}_{1,\sigma}^{\dagger}(j) &:= \hat{f}_{j,\sigma}^{\dagger} \hat{\tau}_{j+\frac{1}{2}}^z \hat{f}_{j+1,\sigma}^{\dagger}. \end{aligned} \quad (15)$$

Here $\hat{\Phi}_{0,0}^{\dagger}$ represents a singlet pair, while the other three ones are triplet pairs. In an antiferromagnetic background, triplet pairing should be suppressed due to a large energy cost. Meanwhile, they also exhibit repulsive interactions in Eq. (14), which are generally irrelevant to the superconductivity. However, the situation is different for singlet pairs, which are low-energy pairings in antiferromagnetic backgrounds and have attractive interactions in \hat{H}_K . Therefore, $\hat{\Phi}_{0,0}$ should be the dominant pairing that contributes to the charge dynamics. Moreover, this term should be also expected to enhance the superconducting instability due to the attractive interaction. Thus we expect a superconducting single phase under large electric fields and proper doping.

V. NUMERICAL SIMULATIONS

To verify the above results, we need to perform numerical simulations. We implement the DMRG algorithm, which is one of the most efficient methods to numerically study 1D quantum many-body systems. We project ground states

to the specific gauge sector by adding a Lagrange multiplier λ_j to the original Hamiltonian, i.e., calculating the Hamiltonian

$$\hat{H}_{\text{num}} := \hat{H} + \sum_j \lambda_j \hat{G}_j. \quad (16)$$

Since $[\hat{G}_j, \hat{H}] = 0$, \hat{H} should have the same eigenstates as \hat{H}_{num} . When $\lambda_j \gg 1$, the ground state of \hat{H}_{num} satisfies $\langle \hat{G}_j \rangle = -1$, which is the ground state of \hat{H} in the $\hat{G}_j = -1$ sector. Here we mainly study how electric fields affect excitations of this system in the presence of large U , i.e., the effect of confinement concerning the 1D Hubbard model. To probe excitations, we need to calculate the corresponding gauge-invariant correlation functions. During the calculation, we choose $\lambda_j = 100$, $t = 1$, and open boundary conditions with system size up to $L = 256$. The maximum bond dimension is $\chi = 600$ and truncation errors $\approx 10^{-7}$. The expectation value of the \mathbb{Z}_2 gauge generator satisfies $|\langle \hat{G}_j \rangle + 1| < 10^{-12}$. We note that, despite the absence of rigorous gauge invariance, this numerical method can naturally extend to study experimental imperfections.

A. Lattice fermions

We first consider the confinement and deconfinement of lattice fermions by introducing a string correlation function [62]:

$$C_{\sigma}^f(i-j) := \left\langle \hat{f}_{i,\sigma}^{\dagger} \left(\prod_{i \leq \ell < j} \hat{\tau}_{\ell+\frac{1}{2}}^z \right) \hat{f}_{j,\sigma} \right\rangle. \quad (17)$$

As shown in Fig. 2(a), for the large U , $C_{\sigma}^f(i-j)$ shows exponential decay in the half-filling case for arbitrary electric fields (including $h = 0$). Thus, the lattice fermion is always confined for finite U , which is consistent with the Mott insulator in this case. For hole-doped systems, when $h = 0$, C_{σ}^f shows a power law decay, indicating a deconfinement of $\hat{f}_{i,\sigma}^{\dagger}$ [see Fig. 2(b)]. However, it becomes confined for finite h , which is consistent with the string tension between holes.

B. Spin sector

For the spinon excitation, we define a spin-exchange correlation function

$$C^s(i-j) := \langle \hat{s}_i^+ \hat{s}_j^- \rangle \quad (18)$$

which is also gauge invariant. Figures 3(a) and 3(b) show that this correlation function has a power-law scaling in both half-filling and hole-doped systems, indicating the existence of deconfined spinon excitations. Moreover, in the half-filling case, Fig. 3(a) shows that the C^s is nearly identical to the spin-exchange correlation function of the 1D Heisenberg model for arbitrary h , indicating that the increase in h can hardly affect the effective Hamiltonian (Heisenberg model).

C. Superconductivity

Now we focus on the superconductivity in hole-doped systems. For 1D spin- $\frac{1}{2}$ fermions, in addition to bond pairs defined in Eq. (15), we can also introduce a site singlet

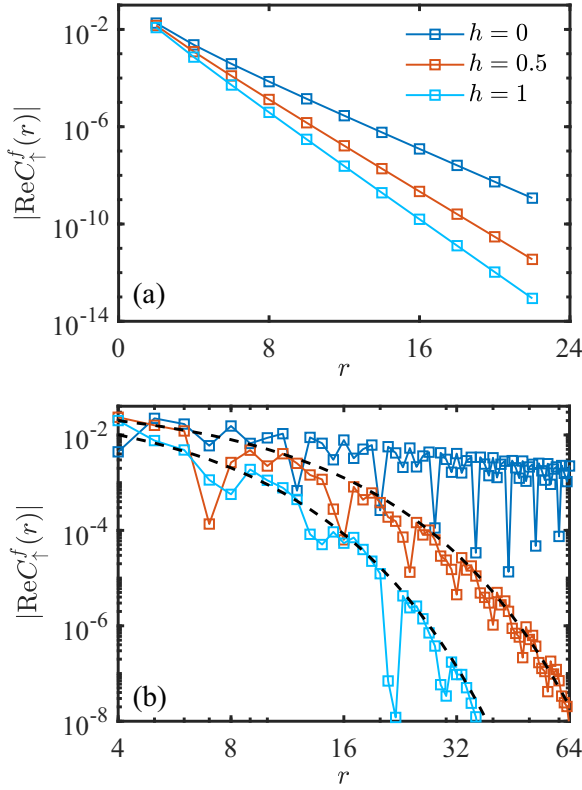


FIG. 2. Correlation functions of lattice fermions $C_f^f(r)$ for (a) 1/2 filling and (b) 3/8 filling, respectively. Here we choose $L = 256$ and $U = 8$. The black dashed curves are fitting exponential functions. To reduce finite-size effects, we calculate the correlation function between sites $L/2$ and $L/2 + r$.

pair $\hat{\Phi}_{SS}^\dagger(j) := \hat{f}_{j,\uparrow}^\dagger \hat{f}_{j,\downarrow}^\dagger$. To study the superconductivity, we need to calculate correlators of the above Cooper pair order parameters, i.e.,

$$C_{\Phi_\alpha}(i-j) := \langle \hat{\Phi}_\alpha^\dagger(i) \hat{\Phi}_\alpha(j) \rangle, \quad (19)$$

where $\alpha = SS/0, 0/1, 0/1, \uparrow/1, \downarrow$. As shown in Fig. 4(a), C_{Φ_α} exhibits an exponential decay for all superconducting order parameters in the case of half filling suggesting the Mott insulator. In Fig. 4(b), we present the result of C_{Φ_α} with 3/8 filling. It shows that all types of Cooper pairs have power-law scalings

$$C_{\Phi_\alpha}(i-j) \sim |i-j|^{-2\Delta_{\Phi_\alpha}}, \quad (20)$$

where Δ_{Φ_α} is the dimension of $\hat{\Phi}_\alpha$. In addition, the bond-singlet pair is indeed the dominant pairing, which is consistent with Eq. (14). Moreover, the dimension of this pair becomes smaller when increasing h [see Figs. 4(c) and 4(d)]. Thus, the electric field can indeed enhance superconductivity, which is consistent with the effective Hamiltonian in Eq. (7).

Now we discuss the dominant order in hole-doped systems. In addition to the superconducting order, two other possible orders in interacting spin- $\frac{1}{2}$ fermion systems are charge density wave (CDW) and spin density wave (SDW). Here, CDW order can be probed by the density-density correlation

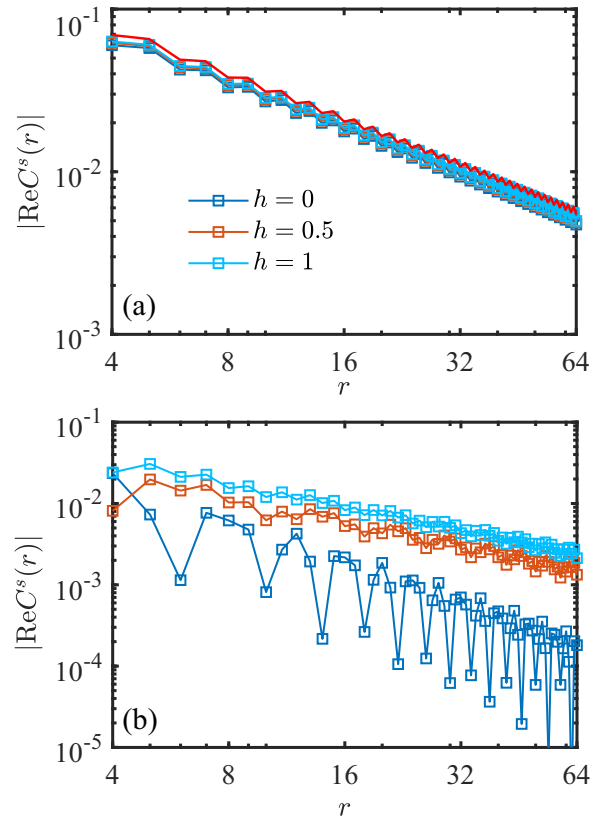


FIG. 3. Correlation functions of spins $C^s(r)$ for (a) 1/2 filling and (b) 3/8 filling, respectively. Here we choose $L = 256$ and $U = 8$. The red line is the spin-exchange correlation function of the 1D Heisenberg model. To reduce finite-size effects, we calculate the correlation function between sites $L/2$ and $L/2 + r$.

function

$$C_N(i-j) := \langle \hat{N}_i \hat{N}_j \rangle - \langle \hat{N}_i \rangle \langle \hat{N}_j \rangle, \quad (21)$$

and the SDW order can be probed by the spin correlation function

$$C_s(i-j) := \langle \hat{s}_i \cdot \hat{s}_j \rangle. \quad (22)$$

In hole-doped systems, similar to the C_{Φ_α} , they also exhibit power-law decay:

$$\begin{aligned} C_N(i-j) &\sim |i-j|^{-2\Delta_{CDW}}, \\ C_s(i-j) &\sim |i-j|^{-2\Delta_{SDW}}, \end{aligned} \quad (23)$$

where Δ_{CDW} and Δ_{SDW} are dimensions of the CDW and SDW, respectively. The most slowly decaying correlation function, i.e., the smallest dimension, means that the corresponding order parameter is dominant in the system.

In Figs. 5(a) and 5(b), we present the dimensions of CDW, SDW, and bond-singlet pairs versus electric fields for different filling factors. When $h = 0$, i.e., the Hubbard model, we can find that Δ_{CDW} and Δ_{SDW} are both smaller than $\Delta_{\Phi_{0,0}}$, so the dominant order in a hole-doped system is not superconductivity. This is consistent with the result obtained by the bosonization method [4,82]. However, when increasing h , the situation becomes different. For instance, in the case of 3/8 filling and $h = 2$, the dimension of bond-singlet pairs

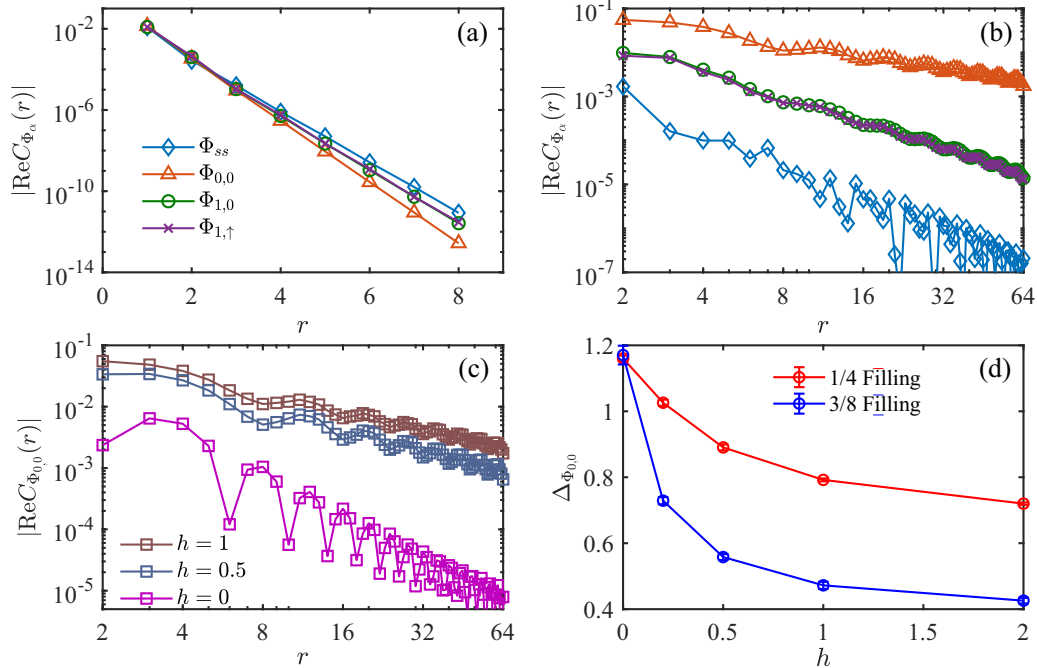


FIG. 4. Correlation functions of superconducting order parameters. (a, b) The scaling of different superconducting order parameters with $h = 1$, $U = 8$, and $L = 256$ in the cases of (a) $1/2$ filling and (b) $3/8$ filling. (c) Correlation functions of bond-singlet pairs for different electric fields. (d) The dimension of bond-singlet pairs versus electric fields. To reduce finite-size effects, we calculate the correlation function $C_{\Phi_\alpha}(r) = \langle \hat{\Phi}_\alpha^\dagger(L/2 + r)\hat{\Phi}_\alpha(L/2) \rangle$.

becomes the smallest one [see Fig. 5(b)]. Therefore, superconducting order can be dominant under the proper doping and large h . In Figs. 5(c) and 5(d), we present the dimensions of the above order parameters versus U for different filling factors. The numerical result shows that the on-site repulsive interaction can enhance the CDW and SDW order, but it weakens the bond-singlet superconducting order. Thus, the electric field term is the relevant term for superconductivity, which is consistent with Eq. (14).

We also study the wave vector of the leading superconducting order parameter, which can be determined by Fourier analysis of the corresponding correlation function [74]

$$S_{\Phi_{0,0}}(k) := \sum_r e^{-ikr} C_{\Phi_{0,0}}(r). \quad (24)$$

Figure 6 shows the absolute value of $S_{\Phi_{0,0}}(k)$ at $3/8$ filling. For small h , there are only two peaks at $k = \pm 2k_F = \pm 3\pi/4$, where $k_F = n\pi$ is the Fermi wave vector with n being the filling factor. However, for large h , we can find that there is a clear leading peak at $k = \pi$ for $|S_{\Phi_{0,0}}(k)|$, with two subleading peaks at $k = \pm 2k_F$. This shows that the dominant superconducting order for the large h is a PDW with π momentum. Therefore, in addition to enhancing the superconducting order, the confinement of lattice fermions can also induce a π momentum.

VI. PROPOSED EXPERIMENTAL IMPLEMENTATION

Finally, we present an approach to realize a 1D \mathbb{Z}_2 LGT coupled to two-component fermions in quantum simulators. According to the above discussion, we know that \hat{H}_U is an

irrelevant term for low-energy physics. Thus, without loss of generality, we just need to consider the Hamiltonian (1) with $U = 0$ in quantum simulations, which is sufficient to demonstrate the above physics. Here we mainly apply an array of spins (or two-level systems) with NN hopping g , where the lattice configuration is shown in Fig. 7. Thus, the original Hamiltonian of this system can be written as

$$\begin{aligned} \hat{H}_{\text{QS}} = & g \sum_j \sum_{\ell=A,B} (\hat{\sigma}_{\ell,j}^+ \hat{\tau}_{j+\frac{1}{2}}^- + \hat{\sigma}_{\ell,j+1}^+ \hat{\tau}_{j+\frac{1}{2}}^- + \text{H.c.}) \\ & + \sum_j (V_A \hat{\sigma}_{A,j}^+ \hat{\sigma}_{A,j}^- + V_B \hat{\sigma}_{B,j}^+ \hat{\sigma}_{B,j}^- + h \hat{\tau}_{j+\frac{1}{2}}^x). \end{aligned} \quad (25)$$

We let the potential of A and B spins satisfy $V_A = -V_B \gg g, h$. Using the Schrieffer-Wolf transformation, we can obtain the effective spin Hamiltonian as

$$\begin{aligned} \hat{H}_e = & \sum_j (g_e \hat{\sigma}_{A,j}^+ \hat{\tau}_{j+\frac{1}{2}}^z \hat{\sigma}_{A,j+1}^- - g_e \hat{\sigma}_{B,j}^+ \hat{\tau}_{j+\frac{1}{2}}^z \hat{\sigma}_{B,j+1}^- + \text{H.c.}) \\ & + h \sum_j \hat{\tau}_{j+\frac{1}{2}}^x, \end{aligned} \quad (26)$$

where $g_e = \lambda^2/V_A$. This is a \mathbb{Z}_2 LGT coupled to two species of spins. To map the Hamiltonian \hat{H}_e to Eq. (1), we first apply a particle-hole transformation of the B spin to change the sign of the coupling between B spins and gauge fields. Then, via a Jordan-Wigner transformation, we can map A/B spins to spin- $1/2$ fermions, and the final Hamiltonian will become Eq. (1) with $U = 0$. Detailed derivations can be found in Appendix B. Generally, the Hamiltonian in Eq. (25) is accessible in various artificial quantum many-body systems, including optical

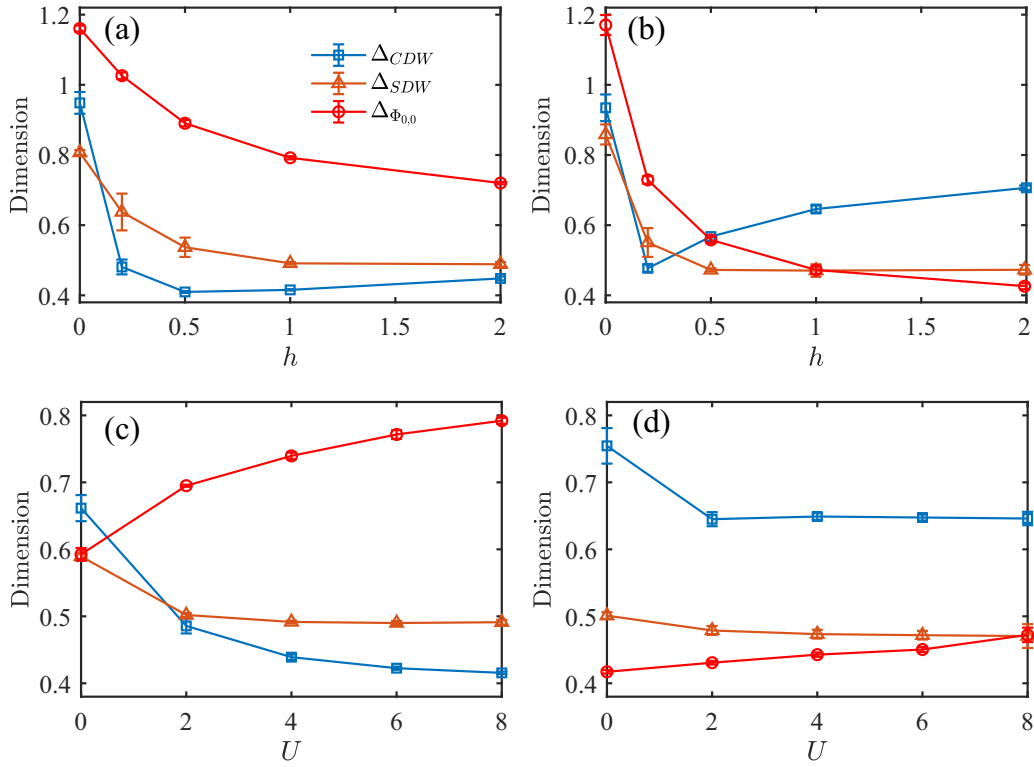


FIG. 5. Dimensions of CDW, SDW, and bond-singlet pairs. (a), (b) Dimensions of these order parameters versus applied electric field h for (a) 1/4 filling and (b) 3/8 filling, respectively. We fix $U = 8$. (c), (d) Dimensions versus U for (c) 1/4 filling and (d) 3/8 filling. We fix $h = 1$.

lattices [21,22,26], Rydberg atoms [27,83], and superconducting circuits [84,85].

VII. SUMMARY AND OUTLOOK

We have systematically studied the ground state of a spin- $\frac{1}{2}$ fermion chain coupled to a \mathbb{Z}_2 LGT. In the $\hat{G}_j = -1$ sector, the model is equivalent to a 1D Hubbard model coupled to

a \mathbb{Z}_2 LGT. At half filling, the system is a Mott insulator, when at least one of h and U is finite, and the spin sector is an antiferromagnetic Heisenberg model with fractionalized spinon excitations. In hole-doped systems, the lattice fermion is confined under nonzero electric fields, leading to the emergence of hole-pair bound states. Remarkably, we also demonstrate that this hole pair can enhance the superconducting instability, and the superconducting order can even be the dominant order for a suitable filling factor and large applied electric field. In addition, the confinement can induce a π momentum for the dominant superconducting order parameter leading to a PDW. We also propose possible experimental realizations of this model in an array of two-level systems. Our results demonstrate that the confinement of lattice fermions can enhance a superconducting instability, which paves the way for understanding unconventional superconductors with \mathbb{Z}_2 LGTs. Meanwhile, our model could also be implemented experimentally in state-of-art quantum simulators [21–27].

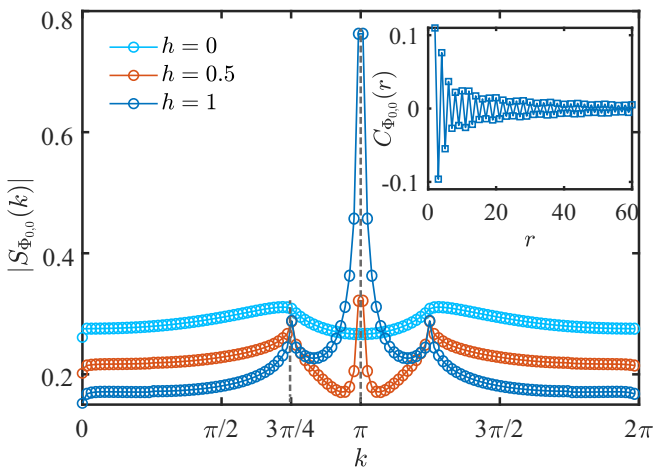


FIG. 6. Fourier analysis of the bond-singlet pair correlation for different h . We choose 3/8 filling and $L = 256$. Inset: The corresponding correlation function in real space for $h = 1$, where there exists an oscillation with a period of two sites.

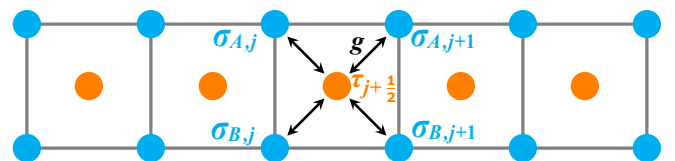


FIG. 7. Lattice skeleton of Eq. (25). Top/bottom blue sites represent A/B spins (matter fields), and orange sites are τ spins (gauge fields). Each τ spin can couple to its four NN σ spins.

The Hamiltonian (1) is reminiscent of the Holstein-Hubbard model [86–88], which is a typical strongly correlated system with both electron-electron and electron-phonon interactions. Thus, studying the relations between LGTs and the Holstein-Hubbard model is a relevant question. Another particularly interesting and natural extension of our paper would be generalizing our model to two dimensions [8–11,69,70,89–91], which might be relevant for understanding high- T_c superconductors. It will also be an interesting issue to consider a ladder model [92], which is one of the simplest cases that open a spin gap [75,93–95].

ACKNOWLEDGMENTS

We thank M. Dalmonte, E. Rinaldi, and R.-Z. Huang for insightful discussions. This work is supported in part by: Nippon Telegraph and Telephone Corporation (NTT) Research, the Japan Science and Technology Agency (JST) via the Quantum Leap Flagship Program (Q-LEAP), and the Moonshot Research and Development (Grant No. JPMJMS2061), the Japan Society for the Promotion of Science (JSPS) via the Grants-in-Aid for Scientific Research (KAKENHI) (Grant No. JP20H00134), the Asian Office of Aerospace Research and Development (AOARD) (Grant No. FA2386-20-1-4069), and the Foundational Questions Institute Fund (FQXi) (Grant No. FQXi-IAF19-06).

APPENDIX A: EFFECTIVE HAMILTONIAN IN THE CASE OF STRONG TENSION

Here we present details of deriving the effective Hamiltonian with the Schrieffer-Wolf transformation [80,81] in the

case of $h \gg t$ and $U \rightarrow 0$. First, we rewrite the Hamiltonian as

$$\begin{aligned}\hat{H} &= \hat{H}_0 + \hat{H}_1, \\ \hat{H}_0 &= -h \sum_j \hat{\tau}_{j+\frac{1}{2}}^x, \\ \hat{H}_1 &= -t \sum_j \sum_{\sigma=\uparrow,\downarrow} (\hat{f}_{j,\sigma}^\dagger \hat{\tau}_{j+\frac{1}{2}}^z \hat{f}_{j+1,\sigma} + \text{H.c.}),\end{aligned}\quad (\text{A1})$$

where \hat{H}_0 is a diagonal term, while \hat{H}_1 is an off-diagonal one. Now, for $h \gg t$, we use the Schrieffer-Wolff transformation [80,81] to obtain the effective Hamiltonian

$$\hat{H}_{\text{eff}} = e^{-\hat{S}} \hat{H} e^{\hat{S}}. \quad (\text{A2})$$

To second order,

$$\begin{aligned}\hat{H}_{\text{eff}} &= \hat{H}_0 + (\hat{H}_1 + [\hat{H}_0, \hat{S}]) + \frac{1}{2}[(\hat{H}_1 + [\hat{H}_0, \hat{S}]), \hat{S}] \\ &\quad + \frac{1}{2}[\hat{H}_1, \hat{S}].\end{aligned}\quad (\text{A3})$$

When this condition holds,

$$\hat{H}_1 + [\hat{H}_0, \hat{S}] = 0, \quad (\text{A4})$$

then the final effective Hamiltonian reads

$$\hat{H}_{\text{eff}} = \hat{H}_0 + \frac{1}{2}[\hat{H}_1, \hat{S}]. \quad (\text{A5})$$

Here we choose the form of \hat{S} as

$$\hat{S} = \frac{it}{2h} \sum_{j,\sigma} (\hat{f}_{j,\sigma}^\dagger \hat{\tau}_{j+\frac{1}{2}}^y \hat{f}_{j+1,\sigma} + \text{H.c.}), \quad (\text{A6})$$

where it is not difficult to verify that it indeed satisfies the condition in Eq. (A4). Thus, we have

$$\begin{aligned}[\hat{H}_1, \hat{S}] &= -\frac{it^2}{2h} \left[\sum_{i,\sigma'} (\hat{f}_{i,\sigma'}^\dagger \hat{\tau}_{i+\frac{1}{2}}^z \hat{f}_{i+1,\sigma'} + \text{H.c.}), \sum_{j,\sigma} (\hat{f}_{j,\sigma}^\dagger \hat{\tau}_{j+\frac{1}{2}}^y \hat{f}_{j+1,\sigma} + \text{H.c.}) \right] \\ &= -\frac{it^2}{2h} \left[\sum_{j,\sigma} (2i\hat{\tau}_{j+\frac{1}{2}}^x)(2\hat{n}_{j,\sigma}\hat{n}_{j+1,\sigma} - \hat{n}_{j,\sigma} - \hat{n}_{j+1,\sigma}) + \sum_j (-4i\hat{\tau}_{j+\frac{1}{2}}^x)(\hat{f}_{j,\uparrow}^\dagger \hat{f}_{j,\downarrow}^\dagger \hat{f}_{j+1,\downarrow} \hat{f}_{j+1,\uparrow} + \text{H.c.}) \right. \\ &\quad \left. + \sum_j (4i\hat{\tau}_{j+\frac{1}{2}}^x)(\hat{f}_{j,\uparrow}^\dagger \hat{f}_{j,\downarrow} \hat{f}_{j+1,\downarrow}^\dagger \hat{f}_{j+1,\uparrow} + \text{H.c.}) + \sum_{j,\sigma} (\hat{\tau}_{j-\frac{1}{2}}^z \hat{\tau}_{j+\frac{1}{2}}^y - \hat{\tau}_{j-\frac{1}{2}}^y \hat{\tau}_{j+\frac{1}{2}}^z)(\hat{f}_{j-1,\sigma}^\dagger \hat{f}_{j+1,\sigma} - \text{H.c.}) \right].\end{aligned}\quad (\text{A7})$$

We define spin operators as

$$\begin{aligned}\hat{s}_j &:= \sum_{\alpha,\beta} \hat{f}_{j,\alpha}^\dagger \sigma_{\alpha\beta} \hat{f}_{j,\beta}, \\ \hat{\eta}_j &:= \hat{P}^{-1} \hat{s}_j \hat{P},\end{aligned}\quad (\text{A8})$$

where \hat{P} corresponds to the particle-hole transformation satisfying

$$\begin{aligned}\hat{P}^{-1} \hat{f}_{j,\uparrow} \hat{P} &= \hat{f}_{j,\uparrow}, \\ \hat{P}^{-1} \hat{f}_{j,\downarrow} \hat{P} &= (-1)^j \hat{f}_{j,\downarrow}^\dagger.\end{aligned}\quad (\text{A9})$$

Hence, we have

$$\begin{aligned}
 \hat{f}_{j,\uparrow}^\dagger \hat{f}_{j,\downarrow} \hat{f}_{j+1,\downarrow}^\dagger \hat{f}_{j+1,\uparrow} + \text{H.c.} &= \hat{s}_j^+ \hat{s}_{j+1}^- + \text{H.c.}, \\
 \hat{f}_{j,\uparrow}^\dagger \hat{f}_{j,\downarrow} \hat{f}_{j+1,\downarrow} \hat{f}_{j+1,\uparrow} + \text{H.c.} &= -(\hat{\eta}_j^+ \hat{\eta}_{j+1}^- + \text{H.c.}), \\
 \sum_{\sigma} 2\hat{n}_{j,\sigma} \hat{n}_{j+1,\sigma} - \hat{n}_{j,\sigma} - \hat{n}_{j+1,\sigma} &= \hat{s}_j^z \hat{s}_{j+1}^z + \hat{\eta}_j^z \hat{\eta}_{j+1}^z.
 \end{aligned} \tag{A10}$$

Therefore, Eq. (A7) can be rewritten as

$$[\hat{H}_1, \hat{S}] = \frac{t^2}{h} \sum_j \hat{\tau}_{j+\frac{1}{2}}^x \cdot (\hat{s}_j \cdot \hat{s}_{j+1} + \hat{\eta}_j \cdot \hat{\eta}_{j+1}) + \frac{-it^2}{2h} \sum_{j,\sigma} (\hat{\tau}_{j-\frac{1}{2}}^z \hat{\tau}_{j+\frac{1}{2}}^y - \hat{\tau}_{j-\frac{1}{2}}^y \hat{\tau}_{j+\frac{1}{2}}^z) (\hat{f}_{j-1,\sigma}^\dagger \hat{f}_{j+1,\sigma} - \text{H.c.}). \tag{A11}$$

According to Eq. (A5), we can obtain the final form of the

effective Hamiltonian:

$$\begin{aligned}
 \hat{H}_{\text{eff}} &= -h \sum_j \hat{\tau}_{j+\frac{1}{2}}^x + J \sum_j \hat{\tau}_{j+\frac{1}{2}}^x \cdot (\hat{s}_j \cdot \hat{s}_{j+1} + \hat{\eta}_j \cdot \hat{\eta}_{j+1}) \\
 &\quad - \frac{iJ}{2} \sum_{j,\sigma} (\hat{\tau}_{j-\frac{1}{2}}^z \hat{\tau}_{j+\frac{1}{2}}^y - \hat{\tau}_{j-\frac{1}{2}}^y \hat{\tau}_{j+\frac{1}{2}}^z) \\
 &\quad \times (\hat{f}_{j-1,\sigma}^\dagger \hat{f}_{j+1,\sigma} - \text{H.c.}),
 \end{aligned} \tag{A12}$$

where $J = t^2/h$. Using the identity

$$\hat{\tau}_{j-\frac{1}{2}}^z \hat{\tau}_{j+\frac{1}{2}}^y - \hat{\tau}_{j-\frac{1}{2}}^y \hat{\tau}_{j+\frac{1}{2}}^z = i\hat{\tau}_{j+\frac{1}{2}}^x \cdot (\hat{\tau}_{j-\frac{1}{2}}^z \hat{\tau}_{j+\frac{1}{2}}^z + \hat{\tau}_{j-\frac{1}{2}}^y \hat{\tau}_{j+\frac{1}{2}}^y), \tag{A13}$$

we can finally obtain the effective Hamiltonian in Eq. (7).

APPENDIX B: PROPOSED EXPERIMENTAL IMPLEMENTATION

Here we show details about how to realize the Hamiltonian (1) in quantum simulators. We consider spin (or two-level) systems with spin exchange coupling, as well as tunable longitudinal and transverse fields. The lattice configuration is shown in Fig. 7, and the original Hamiltonian of this system can be written as

$$\begin{aligned}
 \hat{H}_{\text{QS}} &= \hat{H}_{\text{QS},0} + \hat{H}_{\text{QS},1}, \\
 \hat{H}_{\text{QS},0} &= \sum_j V_A \hat{\sigma}_{A,j}^+ \hat{\sigma}_{A,j}^- + V_B \hat{\sigma}_{B,j}^+ \hat{\sigma}_{A,j}^- - h \hat{\tau}_{j+\frac{1}{2}}^x, \\
 \hat{H}_{\text{QS},1} &= g \sum_j \sum_{\ell=A,B} \hat{\sigma}_{\ell,j}^+ \hat{\tau}_{j+\frac{1}{2}}^- + \hat{\sigma}_{\ell,j+1}^+ \hat{\tau}_{j+\frac{1}{2}}^- + \text{H.c.}
 \end{aligned} \tag{B1}$$

To realize a \mathbb{Z}_2 LGT coupled to a two-component matter field, we let $V_A = -V_B = V \gg g, h$.

We apply the Schrieffer-Wolf transformation to obtain the effective spin Hamiltonian. Similar to Ref. [42], the generating function can be chosen as

$$\begin{aligned}
 \hat{S}' &= \frac{ig}{V} \sum_j \hat{\sigma}_{A,j}^+ \hat{\tau}_{j+\frac{1}{2}}^- + \hat{\sigma}_{A,j+1}^+ \hat{\tau}_{j+\frac{1}{2}}^- \\
 &\quad - \hat{\sigma}_{B,j}^+ \hat{\tau}_{j+\frac{1}{2}}^- - \hat{\sigma}_{B,j+1}^+ \hat{\tau}_{j+\frac{1}{2}}^- - \text{H.c.}
 \end{aligned} \tag{B2}$$

According to Eq. (A5), we can obtain the final effective Hamiltonian of \hat{H}_{QS} as

$$\begin{aligned}
 \hat{H}_e &= \hat{H}_{\text{QS},0} + \frac{1}{2} [\hat{H}_{\text{QS},1}, \hat{S}'] \\
 &= g_e \sum_j (\hat{\sigma}_{A,j}^+ \hat{\tau}_{j+\frac{1}{2}}^z \hat{\sigma}_{A,j+1}^- - \hat{\sigma}_{B,j}^+ \hat{\tau}_{j+\frac{1}{2}}^z \hat{\sigma}_{B,j+1}^- + \text{H.c.}) \\
 &\quad + g_e \sum_j [\hat{\tau}_{j-\frac{1}{2}}^+ (\hat{\sigma}_{B,j}^z - \hat{\sigma}_{A,j}^z) \hat{\tau}_{j+\frac{1}{2}}^- + \text{H.c.}] \\
 &\quad + \sum_j (V + 2g_e) \hat{\sigma}_{A,j}^+ \hat{\sigma}_{A,j}^- + (V - 2g_e) \hat{\sigma}_{B,j}^+ \hat{\sigma}_{B,j}^- - h \hat{\tau}_{j+\frac{1}{2}}^x,
 \end{aligned} \tag{B3}$$

where $g_e = g^2/V$. Here we can find that the total spins of the A and B sublattices are both conserved, i.e., $[\sum_j \hat{\sigma}_{\ell,j}^+ \hat{\sigma}_{\ell,j}^-, \hat{H}_e] = 0$. Thus, the potential terms of A/B spins can be neglected. In addition, for large h , the second term of Eq. (B3) is irrelevant [42]. Therefore, the effective Hamiltonian in this case can be simplified as

$$\begin{aligned}
 \hat{H}_e &= g_e \sum_j (\hat{\sigma}_{A,j}^+ \hat{\tau}_{j+\frac{1}{2}}^z \hat{\sigma}_{A,j+1}^- - \hat{\sigma}_{B,j}^+ \hat{\tau}_{j+\frac{1}{2}}^z \hat{\sigma}_{B,j+1}^- + \text{H.c.}) \\
 &\quad - h \sum_j \hat{\tau}_{j+\frac{1}{2}}^x.
 \end{aligned} \tag{B4}$$

Now we apply a particle-hole transformation of B sites $\hat{P}_B = \prod_{j=\text{odd}} \hat{\sigma}_{B,j}^z$, which can change the sign of the coupling strength between B and τ spins. That is,

$$\begin{aligned}
 \hat{H}_e \rightarrow \hat{P}_B \hat{H}_e \hat{P}_B &= g_e \sum_j (\hat{\sigma}_{A,j}^+ \hat{\tau}_{j+\frac{1}{2}}^z \hat{\sigma}_{A,j+1}^- + \hat{\sigma}_{B,j}^+ \hat{\tau}_{j+\frac{1}{2}}^z \hat{\sigma}_{B,j+1}^- \\
 &\quad + \text{H.c.}) - h \sum_j \hat{\tau}_{j+\frac{1}{2}}^x.
 \end{aligned} \tag{B5}$$

Finally, to map the matter field from spins to fermions, we can use a Jordan-Wigner transformation defined as

$$\begin{aligned}
 \hat{f}_{j,\uparrow}^\dagger &= \hat{\sigma}_{A,j}^+ \prod_{k<j} \hat{\sigma}_{A,k}^z, \\
 \hat{f}_{j,\downarrow}^\dagger &= \hat{\sigma}_{B,j}^+ \prod_{k<j} \hat{\sigma}_{B,k}^z \prod_{l=1}^L \hat{\sigma}_{A,l}^z.
 \end{aligned} \tag{B6}$$

Hence, \hat{H}_e can be mapped to the Hamiltonian in Eq. (1), i.e., a spin- $\frac{1}{2}$ fermion chain minimally coupled to a \mathbb{Z}_2 LGT. We

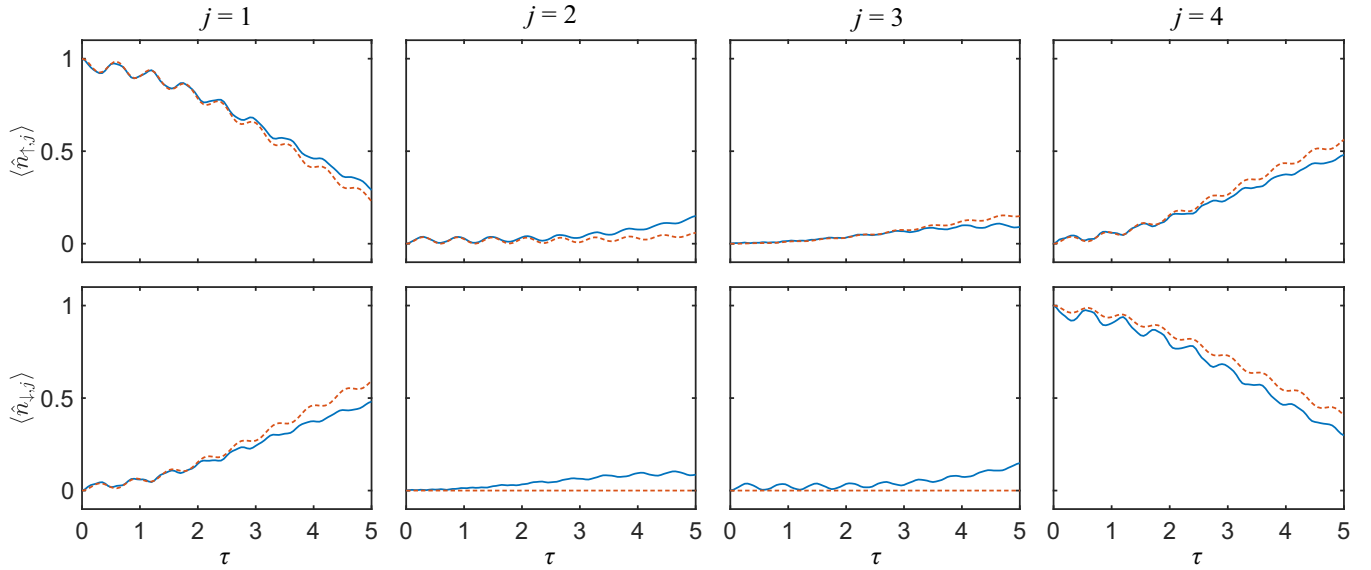


FIG. 8. Quench dynamics of Eqs. (1) and (B1) with $L = 4$ (12 qubits). The horizontal axis is the time τ . The parameters are chosen as $J = 20$, $V = 400$, $t = g_e = 1$, and $h = 5$. We consider periodic boundary conditions. The initial state is $|\psi_0\rangle = |\uparrow + 0 - 0 + \downarrow +\rangle$. Solid and dashed curves represent expectation values of the fermion number operator of the Hamiltonians in Eqs. (1) and (B1), respectively.

also perform a numerical simulation to further demonstrate the above discussion. Here we use exact diagonalization to calculate the quench dynamics of Eqs. (1) and (B1) with $L = 4$ (12 qubits). The parameters chosen are $J = 20$, $V = 400$, $t = g_e = 1$, and $h = 5$. To reduce the boundary effect, we consider periodic boundary conditions. The initial state is $|\psi_0\rangle = |\uparrow + 0 - 0 + \downarrow +\rangle$. As shown in Fig. 8, we can find consistent fermion density results when comparing the dynamics of Eqs. (1) and (B1).

APPENDIX C: NEGATIVE U AT HALF FILLING

In this Appendix, we discuss the phase diagram of the Hamiltonian (1) with negative U at half filling. In the gauge sector $\hat{G}_j = -1$, negative U means antiferromagnetic interactions of electric fields or attractive on-site interactions of fermions. As discussed in Sec. III, due to the confinement of lattice fermions, exciting a double occupation and a hole (called meson) with distance r costs energy $\sim (hr + U)$. When $-U \ll h$, this excitation should be absent in the ground state due to the large energy cost. Thus, the gauge field tends to polarize at $\hat{\tau}_j^x = 1$, and the lattice fermion prefers the single-occupation state, i.e., the system should be a Mott insulator with gapless spin sector. However, when $-U \gg h$, the energy cost of exciting a meson is negative, so double occupations and holes tend to dominate resulting in the freeze of the spin sector, i.e., opening a spin gap. Meanwhile, in this case, $\hat{\tau}^x$ tends to have a staggered distribution to make $\langle \hat{\tau}_{j-\frac{1}{2}}^x \hat{\tau}_{j+\frac{1}{2}}^x \rangle < 0$. Therefore, for fixed h , when increasing $-U$, there should be a quantum phase transition from the Mott insulator (gapless) to the meson condensed phase (gapped).

For large $-U$, since $\hat{\tau}^x$ is expected to have a staggered distribution, the ground state should be dimerized [see Fig. 9(a)]. Thus, the condensation of mesons induces a π momentum, i.e., a spontaneous breaking of the translational symmetry occurs. To study this quantum phase transition, we can choose

the order parameter

$$\hat{m}_x := \frac{2}{N} \sum_j (\hat{\tau}_{2j-\frac{1}{2}}^x - \hat{\tau}_{2j+\frac{1}{2}}^x). \quad (\text{C1})$$

For numerical simulations, to reduce the boundary effect, we obtain the order parameter as $\hat{m}_x = \hat{\tau}_{L/2-\frac{1}{2}}^x - \hat{\tau}_{L/2+\frac{1}{2}}^x$. In Fig. 9(b), we present the expectation values of \hat{m}_x versus $-U$ for $h = 1$ and different system sizes. The numerical result show that the critical point is at $-U_c \approx 2.04$ with critical exponents $\Delta_m \approx 0.33$ and $\nu \approx 2.5$, where Δ_m and ν are the order parameter dimension and correlation length critical exponent, respectively.

To further understand this quantum phase transition, we now focus on the matter field. When $h = 0$, for large $-U$, the lattice fermion at half filling has a gapped spin sector and a gapless charge sector [4,82]. However, according to the above discussion, we find that the charge sector becomes gapped under finite h for large $-U$. In addition, due to the pseudospin rotation symmetry ($SU_\eta(2)$), which cannot be broken spontaneously in 1D systems, this gapped translational symmetry breaking phase cannot be a CDW. Therefore, to preserve the $SU_\eta(2)$ symmetry, we expect that the charge sector is a pseudospin valence-bond solid [see Fig. 9(c)]. This order can be described by the order parameter

$$\hat{v}_\eta := \frac{2}{N} \sum_j (\hat{\eta}_{2j-1} \cdot \hat{\eta}_{2j} - \hat{\eta}_{2j} \cdot \hat{\eta}_{2j+1}). \quad (\text{C2})$$

In Fig. 9(d), we present the expectation values of \hat{v}_η versus $-U$ for $h = 1$ and different system sizes, where we calculate it as $\hat{v}_\eta = \hat{\eta}_{L/2-1} \cdot \hat{\eta}_{L/2} - \hat{\eta}_{L/2} \cdot \hat{\eta}_{L/2+1}$ to reduce the boundary effect. We can find that \hat{v}_η can also represent this quantum phase transition and has the same dimension as \hat{m}_x at the critical point.

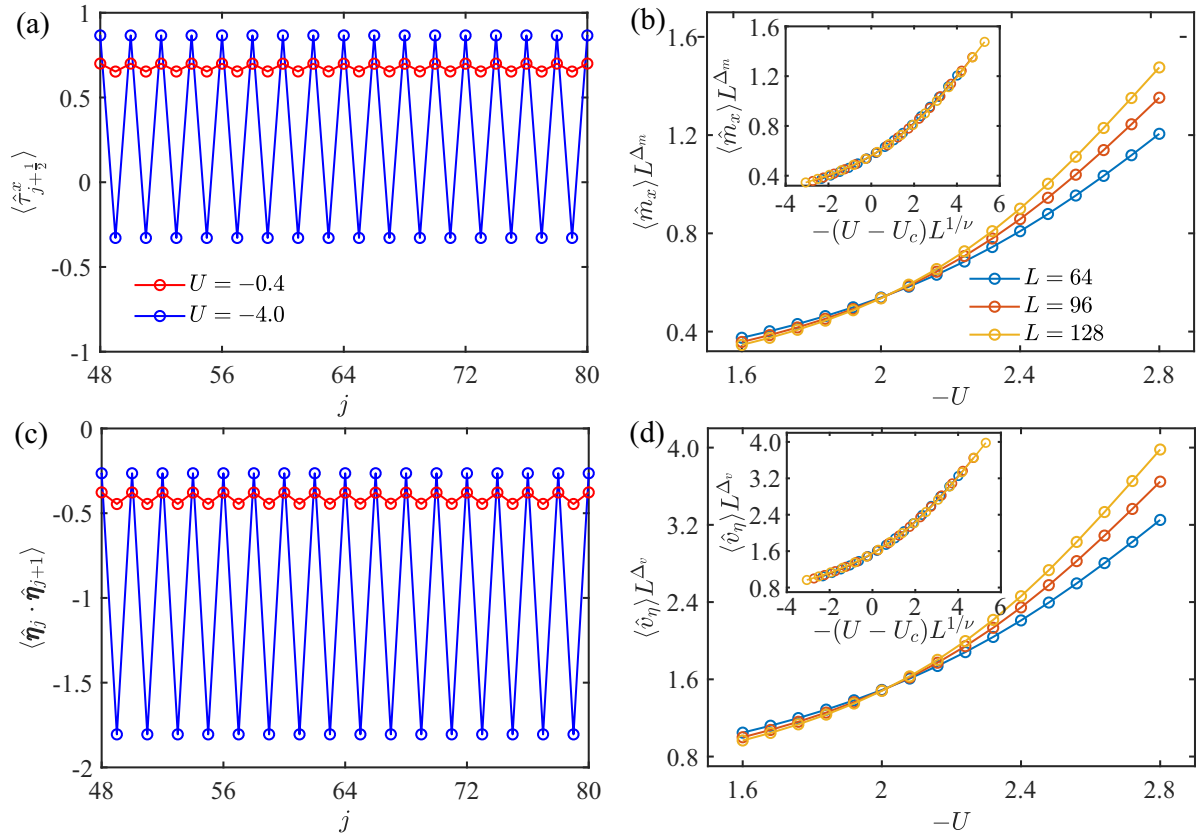


FIG. 9. Quantum phase transition for negative U and $h = 1$ at half filling. (a) Expectation value distributions of $\hat{t}_{j+\frac{1}{2}}^x$ at the ground state for small and large $-U$. (b) Rescaled order parameter $\langle \hat{m}_x \rangle L^{\Delta_m}$ as a function of $-U$ for different system sizes, where the dimension $\Delta_m \approx 0.33$. The curves cross at the critical point $-U_c \approx 2.04$. Inset: The corresponding data collapse with a correlation length critical exponent $\nu \approx 2.5$. (c) Expectation value distributions of $\hat{\eta}_j \cdot \hat{\eta}_{j+1}$ at the ground state for small and large $-U$. (d) Rescaled order parameter $\langle \hat{v}_\eta \rangle L^{\Delta_v}$ as a function of $-U$ for different system sizes, where the dimension $\Delta_v \approx \Delta_m \approx 0.33$. The curves also cross at the critical point. Inset: The corresponding data collapse.

- [1] K. G. Wilson, Confinement of quarks, *Phys. Rev. D* **10**, 2445 (1974).
- [2] J. B. Kogut, An introduction to lattice gauge theory and spin systems, *Rev. Mod. Phys.* **51**, 659 (1979).
- [3] R. Moessner, S. L. Sondhi, and E. Fradkin, Short-ranged resonating valence bond physics, quantum dimer models, and Ising gauge theories, *Phys. Rev. B* **65**, 024504 (2001).
- [4] E. Fradkin, *Field Theories of Condensed Matter Physics* (Cambridge University, Cambridge, England, 2013).
- [5] A. Kitaev, Fault-tolerant quantum computation by anyons, *Ann. Phys. (NY)* **303**, 2 (2003).
- [6] Y. Zhou, K. Kanoda, and T.-K. Ng, Quantum spin liquid states, *Rev. Mod. Phys.* **89**, 025003 (2017).
- [7] T. Senthil, A. Vishwanath, L. Balents, S. Sachdev, and M. P. A. Fisher, Deconfined quantum critical points, *Science* **303**, 1490 (2004).
- [8] G. Baskaran and P. W. Anderson, Gauge theory of high-temperature superconductors and strongly correlated Fermi systems, *Phys. Rev. B* **37**, 580 (1988).
- [9] I. Affleck, Z. Zou, T. Hsu, and P. W. Anderson, SU(2) gauge symmetry of the large- U limit of the Hubbard model, *Phys. Rev. B* **38**, 745 (1988).
- [10] E. Dagotto, E. Fradkin, and A. Moreo, SU(2) gauge invariance and order parameters in strongly coupled electronic systems, *Phys. Rev. B* **38**, 2926 (1988).
- [11] T. Senthil and M. P. A. Fisher, Z_2 gauge theory of electron fractionalization in strongly correlated systems, *Phys. Rev. B* **62**, 7850 (2000).
- [12] E. Manousakis, The spin- $\frac{1}{2}$ Heisenberg antiferromagnet on a square lattice and its application to the cuprous oxides, *Rev. Mod. Phys.* **63**, 1 (1991).
- [13] E. Dagotto, Correlated electrons in high-temperature superconductors, *Rev. Mod. Phys.* **66**, 763 (1994).
- [14] P. A. Lee, N. Nagaosa, and X.-G. Wen, Doping a Mott insulator: Physics of high-temperature superconductivity, *Rev. Mod. Phys.* **78**, 17 (2006).
- [15] D. M. Ceperley, Path integrals in the theory of condensed helium, *Rev. Mod. Phys.* **67**, 279 (1995).
- [16] W. M. C. Foulkes, L. Mitás, R. J. Needs, and G. Rajagopal, Quantum Monte Carlo simulations of solids, *Rev. Mod. Phys.* **73**, 33 (2001).
- [17] R. Mondaini, S. Tarat, and R. T. Scalettar, Quantum critical points and the sign problem, *Science* **375**, 418 (2022).
- [18] S. R. White, Density Matrix Formulation for Quantum Renormalization Groups, *Phys. Rev. Lett.* **69**, 2863 (1992).

- [19] U. Schollwöck, The density-matrix renormalization group, *Rev. Mod. Phys.* **77**, 259 (2005).
- [20] U. Schollwöck, The density-matrix renormalization group in the age of matrix product states, *Ann. Phys. (NY)* **326**, 96 (2011).
- [21] M. Lewenstein, A. Sanpera, V. Ahufinger, B. Damski, A. Sen(De), and U. Sen, Ultracold atomic gases in optical lattices: Mimicking condensed matter physics and beyond, *Adv. Phys.* **56**, 243 (2007).
- [22] I. Bloch, J. Dalibard, and W. Zwerger, Many-body physics with ultracold gases, *Rev. Mod. Phys.* **80**, 885 (2008).
- [23] I. Buluta and F. Nori, Quantum simulators, *Science* **326**, 108 (2009).
- [24] I. Buluta, S. Ashhab, and F. Nori, Natural and artificial atoms for quantum computation, *Rep. Prog. Phys.* **74**, 104401 (2011).
- [25] I. M. Georgescu, S. Ashhab, and F. Nori, Quantum simulation, *Rev. Mod. Phys.* **86**, 153 (2014).
- [26] C. Gross and I. Bloch, Quantum simulations with ultracold atoms in optical lattices, *Science* **357**, 995 (2017).
- [27] A. Browaeys and T. Lahaye, Many-body physics with individually controlled Rydberg atoms, *Nat. Phys.* **16**, 132 (2020).
- [28] T. Byrnes and Y. Yamamoto, Simulating lattice gauge theories on a quantum computer, *Phys. Rev. A* **73**, 022328 (2006).
- [29] E. Zohar, J. I. Cirac, and B. Reznik, Simulating Compact Quantum Electrodynamics with Ultracold Atoms: Probing Confinement and Nonperturbative Effects, *Phys. Rev. Lett.* **109**, 125302 (2012).
- [30] D. Banerjee, M. Dalmonte, M. Müller, E. Rico, P. Stebler, U.-J. Wiese, and P. Zoller, Atomic Quantum Simulation of Dynamical Gauge Fields Coupled to Fermionic Matter: From String Breaking to Evolution after a Quench, *Phys. Rev. Lett.* **109**, 175302 (2012).
- [31] P. Hauke, D. Marcos, M. Dalmonte, and P. Zoller, Quantum Simulation of a Lattice Schwinger Model in a Chain of Trapped Ions, *Phys. Rev. X* **3**, 041018 (2013).
- [32] D. Marcos, P. Rabl, E. Rico, and P. Zoller, Superconducting Circuits for Quantum Simulation of Dynamical Gauge Fields, *Phys. Rev. Lett.* **111**, 110504 (2013).
- [33] G. K. Brennen, G. Pupillo, E. Rico, T. M. Stace, and D. Vodola, Loops and Strings in a Superconducting Lattice Gauge Simulator, *Phys. Rev. Lett.* **117**, 240504 (2016).
- [34] E. Zohar, A. Farace, B. Reznik, and J. I. Cirac, Digital Quantum Simulation of \mathbb{Z}_2 Lattice Gauge Theories with Dynamical Fermionic Matter, *Phys. Rev. Lett.* **118**, 070501 (2017).
- [35] L. Barbiero, C. Schweizer, M. Aidelsburger, E. Demler, N. Goldman, and F. Grusdt, Coupling ultracold matter to dynamical gauge fields in optical lattices: From flux attachment to \mathbb{Z}_2 lattice gauge theories, *Sci. Adv.* **5**, eaav7444 (2019).
- [36] C. Schweizer, F. Grusdt, M. Berngruber, L. Barbiero, E. Demler, N. Goldman, I. Bloch, and M. Aidelsburger, Floquet approach to $\mathbb{Z}(2)$ lattice gauge theories with ultracold atoms in optical lattices, *Nat. Phys.* **15**, 1168 (2019).
- [37] F. Görg, K. Sandholzer, J. Minguzzi, R. Desbuquois, M. Messer, and T. Esslinger, Realization of density-dependent Peierls phases to engineer quantized gauge fields coupled to ultracold matter, *Nat. Phys.* **15**, 1161 (2019).
- [38] B. Yang, H. Sun, R. Ott, H.-Y. Wang, T. V. Zache, J. C. Halimeh, Z.-S. Yuan, P. Hauke, and J.-W. Pan, Observation of gauge invariance in a 71-site Bose-Hubbard quantum simulator, *Nature (London)* **587**, 392 (2020).
- [39] A. Celi, B. Vermersch, O. Viyuela, H. Pichler, M. D. Lukin, and P. Zoller, Emerging Two-Dimensional Gauge Theories in Rydberg Configurable Arrays, *Phys. Rev. X* **10**, 021057 (2020).
- [40] F. M. Surace, P. P. Mazza, G. Giudici, A. Lerose, A. Gambassi, and M. Dalmonte, Lattice Gauge Theories and String Dynamics in Rydberg Atom Quantum Simulators, *Phys. Rev. X* **10**, 021041 (2020).
- [41] Z. Davoudi, M. Hafezi, C. Monroe, G. Pagano, A. Seif, and A. Shaw, Towards analog quantum simulations of lattice gauge theories with trapped ions, *Phys. Rev. Res.* **2**, 023015 (2020).
- [42] Z.-Y. Ge, R.-Z. Huang, Z.-Y. Meng, and H. Fan, Quantum simulation of lattice gauge theories on superconducting circuits: Quantum phase transition and quench dynamics, *Chin. Phys. B* **31**, 020304 (2021).
- [43] D. Paulson, L. Dellantonio, J. F. Haase, A. Celi, A. Kan, A. Jena, C. Kokail, R. van Bijnen, K. Jansen, P. Zoller, and C. A. Muschik, Simulating 2D Effects in Lattice Gauge Theories on a Quantum Computer, *PRX Quantum* **2**, 030334 (2021).
- [44] Z. Wang, Z.-Y. Ge, Z. Xiang, X. Song, R.-Z. Huang, P. Song, X.-Y. Guo, L. Su, K. Xu, D. Zheng, and H. Fan, Observation of emergent \mathbb{Z}_2 gauge invariance in a superconducting circuit, *Phys. Rev. Res.* **4**, L022060 (2022).
- [45] Z.-Y. Zhou, G.-X. Su, J. C. Halimeh, R. Ott, H. Sun, P. Hauke, B. Yang, Z.-S. Yuan, J. Berges, and J.-W. Pan, Thermalization dynamics of a gauge theory on a quantum simulator, *Science* **377**, 311 (2022).
- [46] J. Mildenerger, W. Mruczkiewicz, J. C. Halimeh, Z. Jiang, and P. Hauke, Probing confinement in a \mathbb{Z}_2 lattice gauge theory on a quantum computer, [arXiv:2203.08905](https://arxiv.org/abs/2203.08905).
- [47] L. Homeier, A. Bohrdt, S. Linsel, E. Demler, J. C. Halimeh, and F. Grusdt, Quantum simulation of \mathbb{Z}_2 lattice gauge theories with dynamical matter from two-body interactions in (2+1)D, [arXiv:2205.08541](https://arxiv.org/abs/2205.08541).
- [48] M. Dalmonte and S. Montangero, Lattice gauge theory simulations in the quantum information era, *Contemp. Phys.* **57**, 388 (2016).
- [49] M. C. Banuls, R. Blatt, J. Catani, A. Celi, J. I. Cirac, M. Dalmonte, L. Fallani, K. Jansen, M. Lewenstein, S. Montangero *et al.*, Simulating lattice gauge theories within quantum technologies, *Eur. Phys. J. D* **74**, 165 (2020).
- [50] E. Rinaldi, X. Han, M. Hassan, Y. Feng, F. Nori, M. McGuigan, and M. Hanada, Matrix-Model Simulations Using Quantum Computing, Deep Learning, and Lattice Monte Carlo, *PRX Quantum* **3**, 010324 (2022).
- [51] E. Fradkin and L. Susskind, Order and disorder in gauge systems and magnets, *Phys. Rev. D* **17**, 2637 (1978).
- [52] E. Fradkin and S. H. Shenker, Phase diagrams of lattice gauge theories with Higgs fields, *Phys. Rev. D* **19**, 3682 (1979).
- [53] B. van Heck, E. Cobanera, J. Ulrich, and F. Hassler, Thermal conductance as a probe of the nonlocal order parameter for a topological superconductor with gauge fluctuations, *Phys. Rev. B* **89**, 165416 (2014).
- [54] A. Smith, J. Knolle, D. L. Kovrizhin, and R. Moessner, Disorder-Free Localization, *Phys. Rev. Lett.* **118**, 266601 (2017).
- [55] A. Smith, J. Knolle, R. Moessner, and D. L. Kovrizhin, Absence of Ergodicity without Quenched Disorder: From Quantum Disentangled Liquids to Many-Body Localization, *Phys. Rev. Lett.* **119**, 176601 (2017).

- [56] C. Prosko, S.-P. Lee, and J. Maciejko, Simple \mathbb{Z}_2 lattice gauge theories at finite fermion density, *Phys. Rev. B* **96**, 205104 (2017).
- [57] A. Smith, J. Knolle, R. Moessner, and D. L. Kovrizhin, Dynamical localization in \mathbb{Z}_2 lattice gauge theories, *Phys. Rev. B* **97**, 245137 (2018).
- [58] O. Di Stefano, A. Settineri, V. Macri, L. Garziano, R. Stassi, S. Savasta, and F. Nori, Resolution of gauge ambiguities in ultrastrong-coupling cavity quantum electrodynamics, *Nat. Phys.* **15**, 803 (2019).
- [59] S. Jiang and O. Motrunich, Ising ferromagnet to valence bond solid transition in a one-dimensional spin chain: Analogies to deconfined quantum critical points, *Phys. Rev. B* **99**, 075103 (2019).
- [60] L. Garziano, A. Settineri, O. Di Stefano, S. Savasta, and F. Nori, Gauge invariance of the Dicke and Hopfield models, *Phys. Rev. A* **102**, 023718 (2020).
- [61] D. González-Cuadra, L. Tagliacozzo, M. Lewenstein, and A. Bermudez, Robust topological order in Fermionic \mathbb{Z}_2 gauge Theories: From Aharonov-Bohm Instability to Soliton-Induced Deconfinement, *Phys. Rev. X* **10**, 041007 (2020).
- [62] U. Borla, R. Verresen, F. Grusdt, and S. Moroz, Confined phases of One-Dimensional Spinless Fermions Coupled to \mathbb{Z}_2 Gauge Theory, *Phys. Rev. Lett.* **124**, 120503 (2020).
- [63] U. Borla, R. Verresen, J. Shah, and S. Moroz, Gauging the Kitaev chain, *SciPost Phys.* **10**, 148 (2021).
- [64] M. Kebrič, L. Barbiero, C. Reinmoser, U. Schollwöck, and F. Grusdt, Confinement and Mott Transitions of Dynamical Charges in One-Dimensional Lattice Gauge Theories, *Phys. Rev. Lett.* **127**, 167203 (2021).
- [65] A. Settineri, O. Di Stefano, D. Zueco, S. Hughes, S. Savasta, and F. Nori, Gauge freedom, quantum measurements, and time-dependent interactions in cavity QED, *Phys. Rev. Res.* **3**, 023079 (2021).
- [66] S. Savasta, O. Di Stefano, A. Settineri, D. Zueco, S. Hughes, and F. Nori, Gauge principle and gauge invariance in two-level systems, *Phys. Rev. A* **103**, 053703 (2021).
- [67] U. Borla, B. Jeevanesan, F. Pollmann, and S. Moroz, Quantum phases of two-dimensional \mathbb{Z}_2 gauge theory coupled to single-component fermion matter, *Phys. Rev. B* **105**, 075132 (2022).
- [68] J. C. Halimeh, L. Homeier, H. Zhao, A. Bohrdt, F. Grusdt, P. Hauke, and J. Knolle, Enhancing Disorder-Free Localization through Dynamically Emergent Local Symmetries, *PRX Quantum* **3**, 020345 (2022).
- [69] F. F. Assaad and T. Grover, Simple Fermionic Model of Deconfined Phases and Phase Transitions, *Phys. Rev. X* **6**, 041049 (2016).
- [70] S. Gazit, M. Randeria, and A. Vishwanath, Emergent Dirac fermions and broken symmetries in confined and deconfined phases of \mathbb{Z}_2 gauge theories, *Nat. Phys.* **13**, 484 (2017).
- [71] P. Silvi, E. Rico, M. Dalmonte, F. Tschirsich, and S. Montangero, Finite-density phase diagram of a $(1+1)-d$ non-Abelian lattice gauge theory with tensor networks, *Quantum* **1**, 9 (2017).
- [72] E. Berg, E. Fradkin, S. A. Kivelson, and J. M. Tranquada, Striped superconductors: How spin, charge and superconducting orders intertwine in the cuprates, *New J. Phys.* **11**, 115004 (2009).
- [73] E. Berg, E. Fradkin, and S. A. Kivelson, Theory of the striped superconductor, *Phys. Rev. B* **79**, 064515 (2009).
- [74] E. Berg, E. Fradkin, and S. A. Kivelson, Pair-Density-Wave Correlations in the Kondo-Heisenberg Model, *Phys. Rev. Lett.* **105**, 146403 (2010).
- [75] A. Jaefari and E. Fradkin, Pair-density-wave superconducting order in two-leg ladders, *Phys. Rev. B* **85**, 035104 (2012).
- [76] P. A. Lee, Amperean Pairing and the Pseudogap Phase of Cuprate Superconductors, *Phys. Rev. X* **4**, 031017 (2014).
- [77] E. Fradkin, S. A. Kivelson, and J. M. Tranquada, Colloquium: Theory of intertwined orders in high temperature superconductors, *Rev. Mod. Phys.* **87**, 457 (2015).
- [78] C. N. Yang and S. Zhang, SO_4 symmetry in a Hubbard model, *Mod. Phys. Lett. B* **04**, 759 (1990).
- [79] S. Zhang, Pseudospin Symmetry and New Collective Modes of the Hubbard Model, *Phys. Rev. Lett.* **65**, 120 (1990).
- [80] J. R. Schrieffer and P. A. Wolff, Relation between the Anderson and Kondo Hamiltonians, *Phys. Rev.* **149**, 491 (1966).
- [81] S. Bravyi, D. P. DiVincenzo, and D. Loss, Schrieffer-Wolff transformation for quantum many-body systems, *Ann. Phys. (NY)* **326**, 2793 (2011).
- [82] T. Giamarchi, *Quantum Physics in One Dimension* (Clarendon, Oxford, 2004).
- [83] M. Saffman, T. G. Walker, and K. Mølmer, Quantum information with Rydberg atoms, *Rev. Mod. Phys.* **82**, 2313 (2010).
- [84] J.-Q. You and F. Nori, Atomic physics and quantum optics using superconducting circuits, *Nature (London)* **474**, 589 (2011).
- [85] X. Gu, A. F. Kockum, A. Miranowicz, Y.-X. Liu, and F. Nori, Microwave photonics with superconducting quantum circuits, *Phys. Rep.* **718-719**, 1 (2017).
- [86] J. Zhong and H.-B. Schüttler, Polaronic Anharmonicity in the Holstein-Hubbard Model, *Phys. Rev. Lett.* **69**, 1600 (1992).
- [87] J. Bonča and S. A. Trugman, Bipolarons in the extended Holstein Hubbard model, *Phys. Rev. B* **64**, 094507 (2001).
- [88] Z. Han, S. A. Kivelson, and H. Yao, Strong Coupling Limit of the Holstein-Hubbard Model, *Phys. Rev. Lett.* **125**, 167001 (2020).
- [89] I. Ichinose and T. Matsui, Dynamics of holes and spins in the Hubbard t-J model and high-temperature superconductivity, *Phys. Rev. B* **45**, 9976 (1992).
- [90] A. Nakamura and T. Matsui, Ginzburg-Landau theory of resonating valence bonds and its U(1) phase dynamics, *Phys. Rev. B* **37**, 7940 (1988).
- [91] A. Bohrdt, E. Demler, and F. Grusdt, Rotational Resonances and Regge-like Trajectories in Lightly Doped Antiferromagnets, *Phys. Rev. Lett.* **127**, 197004 (2021).
- [92] J. Nyhegn, C.-M. Chung, and M. Burrello, \mathbb{Z}_N lattice gauge theory in a ladder geometry, *Phys. Rev. Res.* **3**, 013133 (2021).
- [93] E. Dagotto and T. M. Rice, Surprises on the way from one- to two-dimensional quantum magnets: The ladder materials, *Science* **271**, 618 (1996).
- [94] E. Dagotto, J. Riera, and D. Scalapino, Superconductivity in ladders and coupled planes, *Phys. Rev. B* **45**, 5744 (1992).
- [95] D. Poilblanc, D. J. Scalapino, and S. Capponi, Superconducting Gap for a Two-Leg t-J Ladder, *Phys. Rev. Lett.* **91**, 137203 (2003).